Journal of Solid State Chemistry 182 (2009) 2796–2800

Contents lists available at ScienceDirect

Journal of Solid State Chemistry

journal homepage: www.elsevier.com/locate/jssc

Crystallization and second harmonic generation in potassium–sodium niobiosilicate glasses

Antonio Aronne [a,*], Esther Fanelli [a], Pasquale Pernice [a], Simone Peli [b], Claudio Giannetti [b], Gabriele Ferrini [b]

[a] Dipartimento di Ingegneria dei Materiali e della Produzione, Università di Napoli Federico II, Piazzale V. Tecchio, I-80125 Napoli, Italy
[b] Dipartimento di Matematica e Fisica, Università Cattolica del Sacro Cuore, Via dei Musei, 41, I-25121 Brescia, Italy

ARTICLE INFO

Article history:
Received 5 May 2009
Received in revised form
27 July 2009
Accepted 28 July 2009
Available online 4 August 2009

Keywords:
Niobiosilicate glasses
Crystallization
Optical properties
Tungsten-bronze

ABSTRACT

Transparent glasses having molar composition $(23-x)K_2O \cdot xNa_2O \cdot 27Nb_2O_5 \cdot 50SiO_2$ ($x = 0$, 5, 10, 15 and 23) have been synthesized by the melt-quenching technique and their devitrification behaviour has been investigated by DTA and XRD. Depending on the composition, the glasses showed a glass transition temperature in the range 660–680 °C and devitrified in several steps. XRD measurements showed that the replacement of K_2O by Na_2O strongly affects the crystallization behaviour. Particularly, in the glasses with only potassium or low sodium content the first devitrification step is related to the crystallization of an unidentified phase, while in the glass containing only sodium, $NaNbO_3$ crystallizes. For an intermediate sodium content ($x = 10$ and 15) a potassium sodium niobate crystalline phase, belonging to the tungsten-bronze family, is formed by bulk nucleation. This system looks promising to produce active nanostructured glasses as the tungsten-bronze type crystals have ferroelectric, electro-optical and non-linear optical properties. Preliminary measurements evidenced SHG activity in the crystallized glasses containing this phase.

1. Introduction

Second order non-linear optical materials have a wide application field, the main ones being tunable sources on a large spectral range, such as parametric light sources and wavelength converters [1]. Glasses, in spite of their isotropic nature, can be used as suitable materials for non-linear optics, thanks to the possibility to obtain them in a nanostructured state [2–4]. In potassium niobium silicate (KNS) glasses, it was shown that nanostructuring takes place as a consequence of phase separation and can be driven and controlled by proper thermal treatments and/or variation of the composition [5–8]. Consequently, both amorphous and crystalline transparent nanostructures were obtained, with nanocrystals size up to 20 nm. Although from these glasses both binary ($KNbO_3$) and ternary ($KNbSi_2O_7$) phases, showing high non-linear optical activity, may be formed [9], none of them was obtained in nanostructured state [5–8]. In a wide compositional range, unidentified nanocrystals are formed in the early stage of nanostructuring, and afterwards they turn into the same new nanostructured phase by different mechanisms, according to the glass composition [8]. It should be emphasized that the nanostructuring of these phases involves the whole volume of the sample, indicating that bulk nucleation mechanism is the main prerequisite to obtain nanostructuring. Consequently, great interest is devoted to the research of active phases characterized by bulk nucleation.

Besides the well known perovskite crystals, many phases, alkali, mixed alkali and mixed alkali–alkali-heart niobate phases with tetragonal tungsten-bronze structure, as potassium lithium niobate solid solutions (KLN s.s.), have been shown to be potentially a useful material for non-linear optical applications [10–13]. Up to now, such phases have been obtained as single crystals [10–12,14], ceramics [15,16] or films [17].

It was found that the partial substitution of K by Li, in a base glass of molar composition $27K_2O \cdot 27Nb_2O_5 \cdot 46SiO_2$, gave rise to the crystallization from bulk nuclei of KLN s.s. ($K_3Li_2Nb_5O_{15}$) with tungsten-bronze structure [18]. Nevertheless, the replacement of Li over 20 mol% makes more difficult the synthesis of transparent glasses by melt quenching technique, causing spontaneous crystallization of the melt during the cooling. On the other hand, it was reported [19] that the partial replacement of K by Na in KNS glasses does not produce spontaneous crystallization of glasses in a wide composition range. Therefore it is interesting to substitute K by Na in potassium niobium silicate glasses aiming to induce the crystallization of these tungsten-bronze active phases, keeping the advantages of the glass–ceramic process.

* Corresponding author. Fax: +39 08176 82595.
E-mail address: anaronne@unina.it (A. Aronne).

0022-4596/$ - see front matter © 2009 Elsevier Inc. All rights reserved.
doi:10.1016/j.jssc.2009.07.052

In this paper the synthesis, the thermal and crystallization behaviour of K_2O–Na_2O–Nb_2O_5–SiO_2 (KNaNS) glasses, obtained from $23K_2O \cdot 27Nb_2O_5 \cdot 50SiO_2$ base glass by partial substitution of K by Na, are reported. The base glass belongs to the wide KNS glass forming system [6] that has been extensively studied [5,8].

2. Experimental

KNaNS glasses, whose compositions are listed in Table 1, were prepared from reagent grade KNO_3, $NaNO_3$, Nb_2O_5 and SiO_2. Their percentage molar composition can be also expressed by the general formula $(23-x)K_2O \cdot xNa_2O \cdot 27Nb_2O_5 \cdot 50SiO_2$ with $x = 0$, 5, 10, 15 and 23. Well-mixed batches calculated to yield 60 g of glass were melted for 1 h at 1500 °C in Pt crucibles. The melts were quickly poured on a brass plate pre-heated at 400 °C. All glasses were optically transparent and without any crystalline inclusions.

The thermal behaviour of the glasses was studied by differential thermal analysis (DTA). DTA curves were recorded on bulk or powdered (<45 μm) specimens of about 30 mg in air at the heating rate of 10 °C min^{-1}, using a Netzsch thermoanalyser high temperature DSC 404 with Al_2O_3 as reference material. Powdered Al_2O_3 was added to improve heat transfer between bulk samples and sample holder. The temperatures detected on DTA curves are accurate to ±1 K. The heat treatments were performed in the DTA apparatus to eliminate temperature gradients. All the samples for XRD measurements were heat treated in the DTA furnace by quenching them directly after a DTA peak had occurred.

To ascertain the amorphous nature of the initial glasses and to identify the crystalline phases grown during the DTA runs, the thermally processed samples were finely ground and analysed in a computer-assisted X-ray Philips powder diffractometer model PW1710 (Cu$K\alpha$), with a scan speed of 1° min^{-1}.

To study the optical non-linear properties of KNaNS crystallized glass samples, second harmonic generation (SHG) experiments were performed on powdered crystallized samples using a Ti:Sa cavity dumped oscillator emitting infrared radiation at a wavelength of 800 nm (photon energy of 1.57 eV), at a repetition rate of 360 kHz and a maximum energy per pulse of 50 nJ. The infrared radiation was focused onto the powdered (<45 μm) samples using a 40X microscope objective, with a focus diameter of 1.5±0.1 μm. The same microscope objective served as a collecting lens for the SHG radiation (at a wavelength of 400 nm) emitted from the sample. The infrared radiation and its second harmonic were separated by a dichroic mirror (see Fig. 3A) and an optically shielded phototube was used to detect the second harmonic radiation, after further filtering with a dichroic filter (with a 10 nm band pass around 400 nm and an extinction ratio of 10^{-4}). As a reference for SHG measurements, a β-BaB_2O_4 (BBO) crystalline sample was prepared by crystallization of a $48BaO \cdot 48B_2O_3 \cdot 4SiO_2$ glass [20]. All SHG efficiency measurements are relative to the powdered BBO sample.

Table 1
Glass transition and peaks temperature (°C) evaluated from DTA curves recorded at 10 °C min^{-1}.

Sample	x/Na_2O (mol%)	T_g (°C)	T_{lexo} (°C)	$T_{lexo}-T_g$ (°C)	ΔT_{lexo}
Initial glass	0	680	755	75	
Initial glass	5	670	753	83	
Initial glass	10	660	786	77	
Heated 10 h T_g			752		34
Initial glass	15	655	772	117	
Heated 10 h T_g			744		28
Initial glass	23	660	775	108	
Heated 10 h T_g			746		29

3. Results and discussion

All the obtained glasses were transparent and homogeneous. DTA curves of bulk initial glasses are displayed in Fig. 1 and the thermal data are summarized in Table 1. The DTA curves exhibit a slope change that can be related to the glass transition. The inflection point at the slope change on the DTA curves was taken as the glass transition temperature, T_g (Table 1). The reproducibility of T_g values was 2 K. The values of T_g slowly decrease increasing sodium content from 680 °C for $x = 0$–655 °C for $x = 15$ and then the T_g slightly increases (660 °C) for the glass with only sodium $x = 23$.

The bulk samples of the initial glasses devitrify in more steps. All DTA curves show two exothermic peaks in the temperature range from T_g to 1150 °C, except for the $x = 5$ that shows a more complex devitrification behaviour with several overlapped exothermic peaks. As this work is mainly aimed to obtain

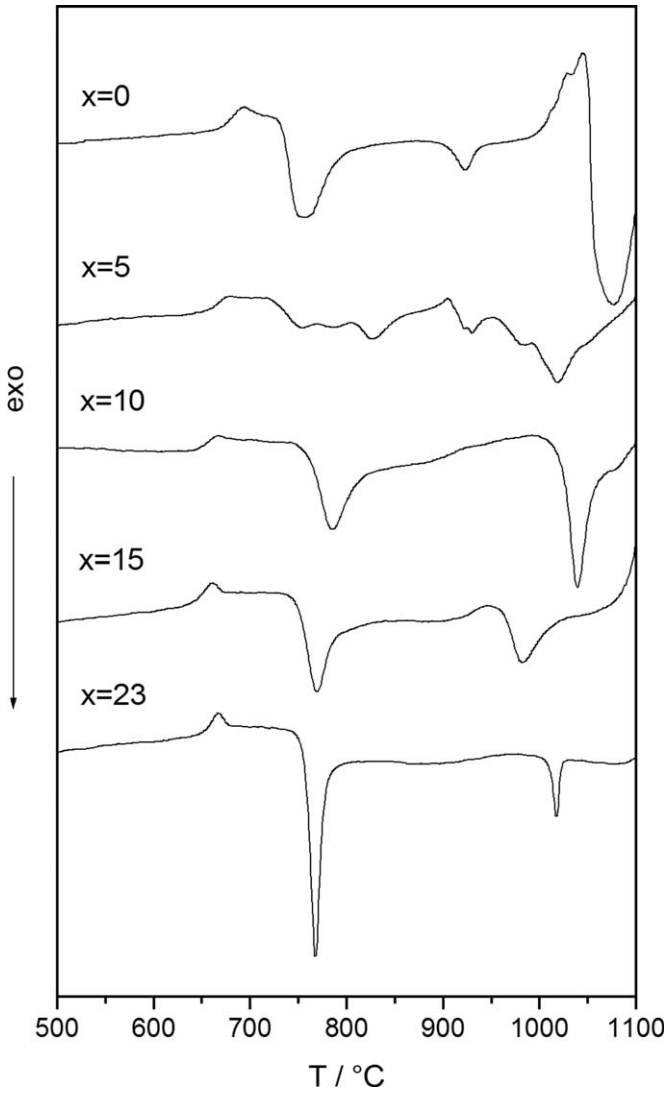

Fig. 1. DTA curves in air at 10 °C min^{-1} of the bulk initial glasses.

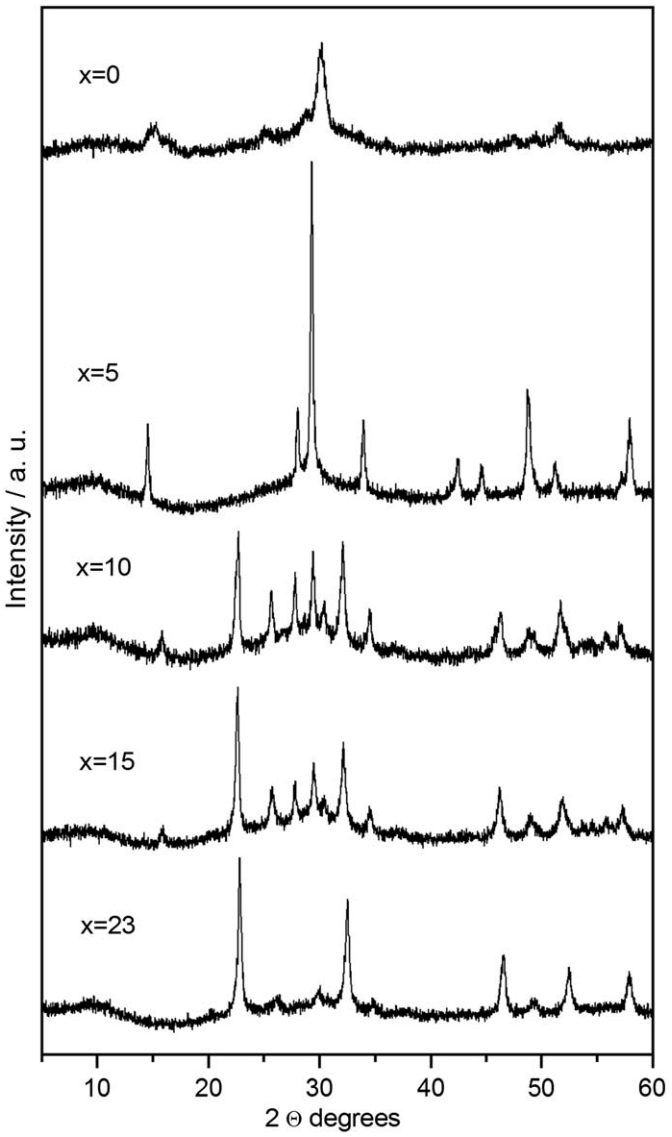

Fig. 2. XRD patterns of the bulk initial glasses heated up to the end temperature of the first DTA exothermic peak and slowly cooled.

nanostructured glasses, the attention will be devoted to the study of the transformations occurring just above the glass transition range, in correspondence of the first exothermic peak.

Bulk samples of each composition were heated at 10 °C min^{-1} in the DTA furnace up to the end temperature of the respective first DTA peak, then quenched to room temperature and analysed by XRD (Fig. 2). These samples hereafter will be denoted by the label indicating the glass composition followed by *−Iexo*.

The heating in the DTA furnace (*Iexo*) produces different effects on the glasses. The $x = 0$*−Iexo* sample keeps its transparency, while the others become opaque. The analysis of the XRD profiles of the $x = 0$*−Iexo* and 5*−Iexo*, Fig. 2, shows that the precipitation in the amorphous matrix of crystallites of unidentified phases takes place, as occurred also for others KNS glasses [5,6,8].

The XRD profile of the $x = 23$*−Iexo*, Fig. 2, shows just five peaks at $2\Theta = 22.7°$, 32.4°, 46.4°, 52.4° and 57.8°, matching $NaNbO_3$ crystal (ICDD 19-1221). Instead, the XRD profiles of the $x = 10$*−Iexo* and 15*−Iexo*, Fig. 2, are quite similar: they display five intense peaks at $2\Theta = 22.7°$, 32.3°, 46.3°, 52.0° and 57.4° together with less intense others. These profiles match $K_3Li_2Nb_5O_{15}$ crystal (ICDD 52-0157), having tetragonal tungsten-bronze structure (TTB) [21]. Similar XRD spectra are reported for many tungsten-bronze phases and were also found in crystallized KLiNS glasses of close composition [18]. The phases belonging to the tungsten-bronze family have tetragonal structure and general formula $(A1)_2(A2)_4C_4(B1)_2(B2)_8O_{30}$, where the *A*1 site is 12-coordinated, the *A*2 and *C* sites are 9-coordinated and both *B* sites are 6-coordinated [14]. The five kinds of sites available to be filled by the different atoms allow the formation of many isomorphous crystals with widely varying ferroelectric and electro-optical properties. Many phases, both stoichiometric and non-stoichiometric, belong to this family, including niobate and tantalate of alkali, mixed alkali and mixed alkali–alkali heart metals.

Although no mixed sodium–potassium niobate TTB phases have been reported in the literature so far, the XRD profiles displayed in Fig. 2 traces (c) and (d) indicate that a mixed sodium–potassium niobate TTB phase crystallizes from KNaNS glasses with $x = 10, 15$.

The SHG activity of the crystallizing phases (tungsten-bronze mixed potassium–sodium niobate and sodium niobate) was measured on crystallized glass samples. The glasses with $x = 10$, 15 and 23 were allowed to crystallize by heating up to the end

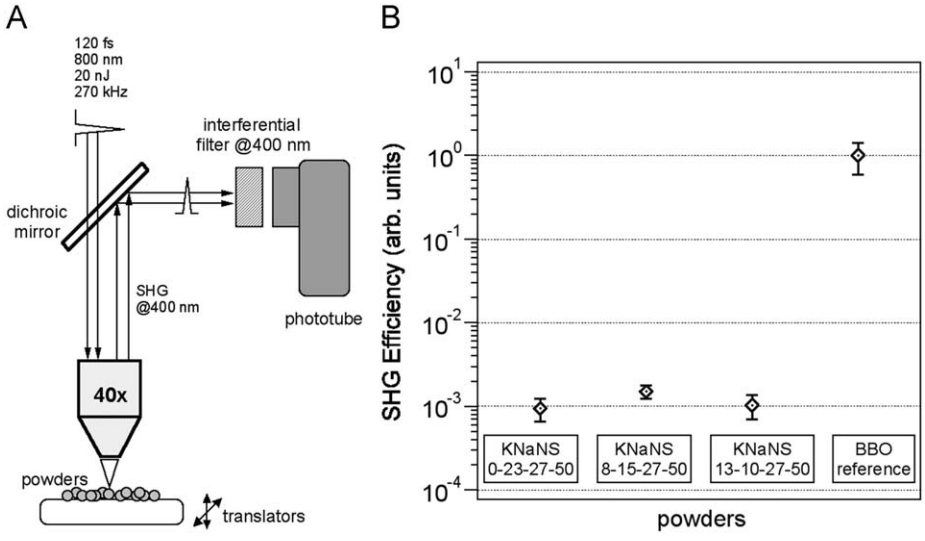

Fig. 3. (A) Scheme of the experimental set-up (B) SHG efficiency relative to BBO of NaNS and KNaNS crystallized glasses, based on $NaNbO_3$ and tungsten-bronze KNaN solid solution, respectively. Each data point in the graph is the average over 10 measurements taken in different spots on the sample.

temperature of the first exothermic DTA peak and powdered. In Fig. 3 the average SHG efficiency of KNaNS crystallized glass samples are reported, with respect to the powdered BBO crystal. The efficiency data are averaged over measurements taken in 10 different spots of the powdered samples, the error bars showing the standard deviation of the SHG signal variation. The obtaining of SHG active phases from KNaNS glasses just above T_g makes these glasses promising to produce nanostructured glasses with SHG activity.

In order to obtain transparent nanostructured glasses with SHG activity, it is necessary that the active crystalline phase grows from the glass exclusively with a bulk nucleation mechanism, without any surface crystallization. This allows, by means of a proper nucleation heat treatment, to produce a high number of bulk nuclei and, consequently, a high number of nanocrystals small enough to avoid any light scattering.

The crystallization mechanism of the KNaNS glasses with $x = 10$, 15 and 23 was consequently investigated. Firstly, the glass samples were subjected to heat treatments in the temperature range close to T_g, where, generally, there is the maximum of the nucleation rate [22]. In this way the occurrence of bulk nucleation can be tested. As known, devitrification is the result of nucleation and crystal growth processes. In a glass the total number of nuclei, N, is the sum of surface nuclei, N_s, bulk nuclei formed during the DTA run, N_h, and bulk nuclei formed during a previous nucleation heat treatment, N_n. The values of N_s, N_h and N_n are respectively proportional to the specific surface area, to the reciprocal of the DTA heating rate and to the time of the nucleation heat treatment. For a given heating rate, the higher the total number of nuclei, N (bulk and/or surface), the lower the temperature of the maximum of the DTA exothermic peak, T_p, according to the following equation: $\ln N = a(1/T_p)+b$, where a and b are constant [22,23].

In our case, the more suitable heat treatment was a 10 h heating at T_g, hence DTA curves of samples previously subjected to this heat treatment are also reported in Fig. 4. Moreover, to investigate the effect of the specific surface area on the devitrification process, DTA curves were also recorded on initial powdered glass samples ($<45\,\mu m$), Fig. 4. The comparison of the heat treated samples with the initial glasses, show that the first exothermic peak is shifted to lower temperature for all the three glasses: $x = 10$ (34 °C), $x = 15$ (28 °C) and $x = 23$ (29 °C), last column in Table 1. On the other hand for powdered samples, the peak temperature remains unchanged.

After the heat treatment, the glass samples are still fully amorphous (XRD, not reported). The DTA curves in Fig. 4 show that, for all the glasses, the heat treated samples keep the same T_g of the initial ones, and, even if the first exothermic peak shifts toward lower temperature, the kind of crystallizing phase is unchanged with respect to the initial glass samples (XRD, not reported). This means that the 10 h heat treatment produces exclusively bulk nucleation process of the TTB phase ($x = 10$ and 15) and of the $NaNbO_3$ ($x = 23$) making them very promising for obtaining transparent nanostructured glasses with SHG activity, although further investigations are needed to optimize the glass compositions and thermal treatments conditions.

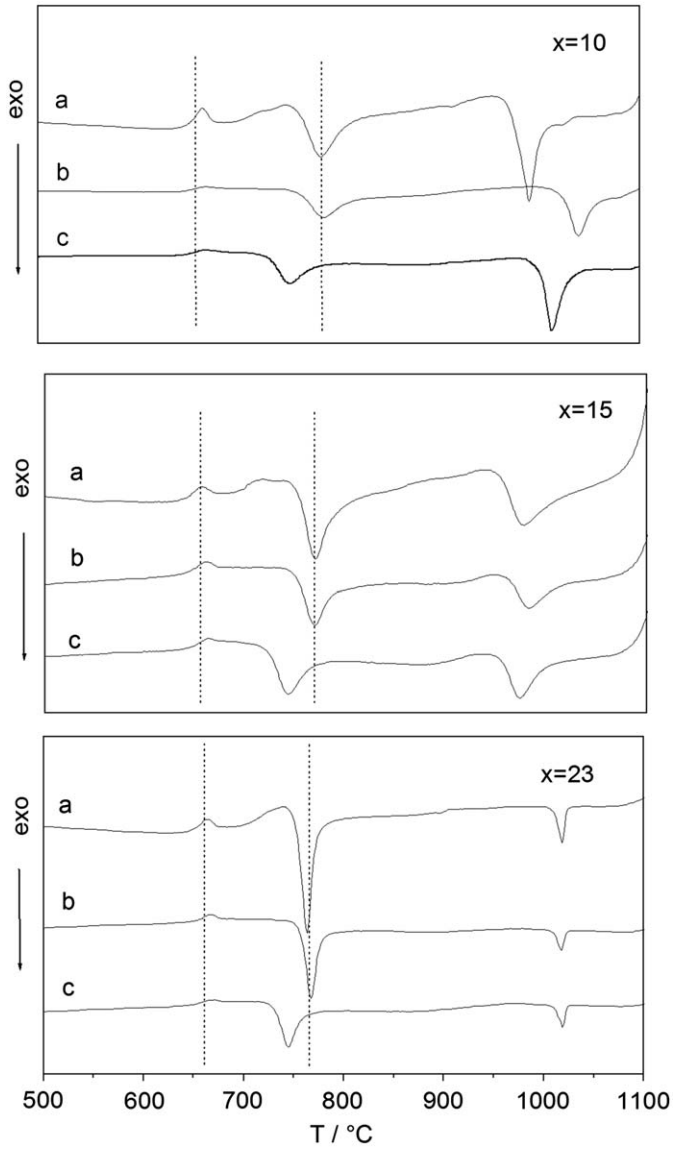

Fig. 4. DTA curves in air at 10 °C min^{-1} of the powdered initial glasses (a), of the bulk initial glasses (b) and of the bulk glasses isothermally heat treated 10 h at T_g (c).

4. Conclusions

The substitution of K_2O by Na_2O strongly affects the crystallization behaviour of the glasses. In the glass without sodium added and for low Na_2O content (5 mol%), just above the glass transition, only crystals of an unidentified phase are formed as in others KNS glasses. At higher Na content, binary alkali niobate crystallizes as the first crystalline phase just above the glass transition. In both the glasses with Na_2O 10 and 15 mol%, KNaN solid solution with tungsten-bronze structure crystallizes from bulk nuclei. This crystalline phase has never been reported in literature until now and it has been obtained by glass crystallization here for the first time. When potassium is fully replaced by sodium, bulk crystallization of $NaNbO_3$ occurs. The crystallized glasses based on tungsten-bronze KNaN solid solution and on $NaNbO_3$ exhibit SHG activity.

The partial replacing of K by Na in KNS glasses makes it possible to obtain transparent nanostructured glasses based on tungsten-bronze mixed alkali niobate nanocrystals showing SHG.

Acknowledgment

This research has been funded by the Italian Ministry of University and Research through the PRIN-2006 project 2006-099419.

References

[1] W. Nie, Adv. Mater. 5 (1993) 520–545.
[2] V.N. Sigaev, S.Yu. Stefanovich, B. Champagnon, I. Gregora, P. Pernice, A. Aronne, R. LeParc, P.D. Sarkisov, C. Dewhurst, J. Non-Cryst. Solids 306 (2002) 238–248.
[3] R.T. Hart, M.A. Anspach, B.J. Kraft, J.M. Zaleski, J.W. Zwanziger, P.J. De Santo, B. Stein, J. Jacob, P. Thiyagarajan, Chem. Mater. 14 (2002) 4422–4429.
[4] S.E. Skipetrov, Nature 432 (2004) 285–286.
[5] P. Pernice, A. Aronne, V.N. Sigaev, M. Kupriyanova, J. Non-Cryst. Solids 275 (2000) 216–224.
[6] A. Aronne, V.N. Sigaev, P. Pernice, E. Fanelli, L.Z. Usmanova, J. Non-Cryst. Solids 337 (2004) 121–129.
[7] A. Aronne, V.N. Sigaev, B. Champagnon, E. Fanelli, V. Califano, L.Z. Usmanova, P. Pernice, J. Non-Cryst. Solids 351 (2005) 3610–3618.
[8] P. Bergese, I. Alessandri, E. Bontempi, L.E. Depero, A. Aronne, E. Fanelli, P. Pernice, T. Boffa Ballaran, N. Miyajima, V.N. Sigaev, J. Phys. Chem. B 110 (2006) 25740–25745.
[9] H. Tanaka, M. Yamamoto, Y. Takahashi, Y. Benino, T. Fujiwara, T. Komatsu, Opt. Mater. 22 (2003) 71–79.
[10] Y. Wan, X. Guo, J. Chen, X. Yuan, J. Chu, J. Li, J. Cryst. Growth 235 (2002) 248–252.
[11] W.W. Xu, T.C. Chong, L. Li, H. Kumagai, M. Hirano, J. Cryst. Growth 198/199 (1999) 536–541.
[12] S. Podlojenov, J. Stade, M. Burianek, M. Muehlberg, Cryst. Res. Technol. 41 (2006) 344–348.
[13] M.N. Ahamad, S. Mizuno, T. Komatsu, K.B.R. Varma, J. Cryst. Growth 304 (2007) 270–274.
[14] S.C. Abrahams, P.B. Jamieson, J.L. Bernstein, J. Chem. Phys. 54 (1971) 2355–2364.
[15] T. Ikeda, K. Kiyohashi, Jpn. J. Appl. Phys. 9 (1970) 1541–1542.
[16] Y.D. Juang, Solid State Commun. 120 (2001) 25–28.
[17] S.K. Park, Thin Solid Films 457 (2004) 397–401.
[18] A. Aronne, E. Fanelli, V. Califano, A. Fragneto, A. Vergara, V.N. Sigaev, P. Pernice, J. Non-Cryst. Solids 354 (2008) 5041–5046.
[19] D.E. Vernacotola, S. Chatlani, J.E. Shelby, in: Proceedings of 2000 IEEE, Twelfth International Symposium on Application of Ferroelectrics, Honolulu, HI, US, July 21–August 2, 2000, pp. 829–832.
[20] A. Aronne, S. Esposito, P. Pernice, Phys. Chem. Glasses 39 (1998) 4–8.
[21] F. Takusagawa, R.A. Jacobson, J. Solid State Chem. 18 (1976) 163–174.
[22] A. Aronne, M. Catauro, P. Pernice, Thermochim. Acta 259 (1995) 269–275.
[23] A. Marotta, P. Pernice, A. Aronne, A. Buri, J. Non-Cryst. Solids 127 (1991) 159–164.